

1955a, U.S. P.
60/064539

Class	Subclass
-------	----------

ISSUE CLASSIFICATION
SCANNED

2663
#11

SERIAL NUMBER 60/064,539 PROVISIONAL	FILING DATE 11/05/97	CLASS	SUBCLASS	GROUP ART UNIT	EXAMINER
--	-------------------------	-------	----------	----------------	----------

APPLICANTS BORIS I. YAKOBSON, RALEIGH, NC.

CONTINUING DATA***
VERIFIED

FOREIGN APPLICATIONS***
VERIFIED

FOREIGN FILING LICENSE GRANTED 04/08/98

Foreign priority claimed 35 USC 119 conditions met	<input type="checkbox"/> yes <input type="checkbox"/> no	AS FILED	STATE OR COUNTRY	SHEETS DRWGS.	TOTAL CLAIMS	INDEP. CLAIMS	FILING FEE RECEIVED	ATTORNEY'S DOCKET NO.
Verified and Acknowledged	Examiner's Initials	→	NC	6			\$150.00	5051-416

ADDRESS

KENNETH D SIBLEY
MYERS BIGEL SIBLEY & SAJOVED
P O BOX 37428
RALEIGH NC 27627

TITLE

INTRAMOLECULAR PLASTICITY AND DUCTILE-BRITTLE RELAXATION IN CARBON
NANOTUBES

U.S. DEPT. OF COMM./PAT. & TM—PTO-436L (Rev. 12-9

Form **SCAN 5** BW
(Rev. 5/97) QC DW

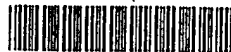
12/

60/064539



11/05/97

PATENT APPLICATION



60064539

Date
Entered
or
Counted

CONTENTS

Date
Received
or
Mailed

1. Application _____ papers.

2. *Request for*

3.

4.

5.

6.

7.

8.

9.

10.

11.

12.

13.

14.

15.

16.

17.

18.

19.

20.

21.

22.

23.

24.

25.

26.

27.

28.

29.

30.

31.

32.

A/PROV

11/05/97
10556 U.S. PRO.

Attorney's Docket No. 5051-416

PATENT

COVER SHEET FOR FILING PROVISIONAL PATENT APPLICATION

Box Provisional Application
Assistant Commissioner for Patents
Washington, DC 20231

This is a request for filing a PROVISIONAL PATENT APPLICATION under 37 C.F.R. § 1.53(b)(2).

Docket No.	5051-416
Type a plus sign (+) inside this box →	+

INVENTOR(s)/APPLICANT(s)

Name: **Boris I. Yakobson**
Residence: **Raleigh, North Carolina**

TITLE OF THE INVENTION (280 characters maximum)

INTRAMOLECULAR PLASTICITY AND DUCTILE-BRITTLE
RELAXATION IN CARBON NANOTUBES

CORRESPONDENCE ADDRESS

Kenneth D. Sibley
Registration No. 31,665
Myers Bigel Sibley & Sajovec
PO Box 37428
Raleigh NC 27627
Tel. (919) 854-1400
Fax (919) 854-1401

ENCLOSED APPLICATION PARTS (check all that apply)

- ☒ Specification (Number of Pages 15)
- ☒ Drawing(s) (Number of Sheets 6)
- ☐ Claims (Number of Claims)
(A complete provisional application does not require claims 37 C.F.R. § 1.51(a)(2).)
- ☐ Small Entity Statement
- ☐ Other (specify)

60064539-110597

In re: Yakobson
Filed: Concurrently Herewith
Page 2

METHOD OF PAYMENT (check one)

- ☒ Check or money order is enclosed to cover the filing fee.
☐ The Commissioner is hereby authorized to charge filing fees and credit Deposit Account No.
☒ Please charge Deposit Account No. 50-0220 for any fee deficiency.

PROVISIONAL FILING FEE AMOUNT(s)

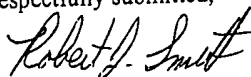
Large Entity \$150.00
Small Entity \$ 75.00

Filing Fee Amount: \$75.00

The invention was made by an agency of the United States Government or under a contract with an agency of the United States Government.

- ☒ No.
☐ Yes, the name of the U.S. Government agency and the Government contract number are:

Respectfully submitted,



Robert J. Smith

Registration No. 40,820

Date: November 5, 1997

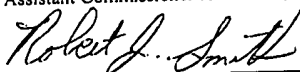
Myers Bigel Sibley & Sajovec
PO Box 37428
Raleigh NC 27627
Tel. (919) 854-1400
Fax (919) 854-1401

CERTIFICATE OF EXPRESS MAIL

"Express Mail" mailing label number EM380380674US

Date of Deposit: November 5, 1997

I hereby certify that this paper or fee is being deposited with the United States Postal Service "Express Mail Post Office to Addressee" service under 37 CFR 1.10 on the date indicated above and is addressed to Box Provisional Application, Assistant Commissioner for Patents, Washington, DC 20231.



Robert J. Smith

Date of Signature: November 5, 1997

60064539-110597

INTRAMOLECULAR PLASTICITY AND DUCTILE-BRITTLE RELAXATION IN CARBON NANOTUBES

Specification

Tubular carbon molecules (nanotubes) possess unique hollow structure and unusual properties. Electronic, chemical-synthetic, mechanical, and some other aspects of nanotubes have attracted attention. Nanotubes derive their band structure from the combination of hexagonal symmetry of graphene sheet and the way it is folded into a cylinder. The latter is usually characterized by the rollup vector $c=(c_1, c_2)$ which becomes the circumference of the nanotube. The helicity vector determines either that the nanotube is metallic or semiconducting. In contrast, the elastic response to mechanical stimuli depends very little on nanotube helicity. The reason for that lies in the fact that the linear elasticity of a two-dimensional hexagonal crystal is strictly isotropic. Carbon nanotubes have already demonstrated exceptional mechanical properties: their high stiffness combines with resilience and the ability to reversibly buckle and collapse. However, the ultimate mechanisms of failure of these molecular structures under extreme tension and thermal load remain a subject of keen fundamental and practical interest. The analysis below begins with the continuum dislocation theory (Sec. 1), but then reveals the atomistics of mechanical relaxation (Secs. 2-3). The sequence of atomic rearrangements corresponds to either brittle cleavage or, at very high temperatures, to a possible "plastic flow" (Sec. 4-5). The latter leads to a stepwise ("quantized") necking, when the domains of different helicity (and different electrical properties) may alternate (Sec. 6). Several corollaries of the theory are discussed (Sec. 6).

1. STRESS FIELD ANALYSIS

Locally, the wall of a nanotube differs very little from a single graphene sheet, a two-dimensional crystal of carbon. Typically, for a diameter d , the curvature adds $0.08 \text{ eVnm}^2/d^2$ of strain energy, and for most diameters it is less than one percent of the binding energy, 7.4 eV per atom. In a perfect crystal lattice such as the wall of a nanotube, a yield to a great axial tension σ (N/m, due to the two-dimensional nature of the nanotube wall, it is convenient here to use force per unit length of the circumference)

begins with a homogeneous nucleation of a slip by the shear stress present. A possible glide of an edge dislocation reduces the total energy, as characterized by the elastic force f on this dislocation. The magnitude of this force is given by the Peach-Koehler equation relating the Burgers vector \mathbf{b} , stress tensor σ , and the dislocation line direction \mathbf{n} ,

$$f_k = -\epsilon_{ijk} n_i \sigma_{jl} b_l, \quad (1)$$

where ϵ_{ijk} is the Levi-Civita permutation symbol, with the components equal to ± 1 or 0 . With the local coordinates x, y , and z chosen along the tube circumference, the axis, and the local normal to the surface correspondingly, one can immediately simplify this equation. Indeed, the edge dislocation "line" can only be normal to the graphene plane, so that $i = z$. Further, the axial tensile stress has only one non-zero component $\sigma_{yy} = \sigma$, therefore $j = l = y$, and $f_k = -\delta_{xk} \sigma b_y$ - the force is always directed *circumferentially* ($k=x$), while its magnitude is proportional to the *axial* component of Burgers vector. Neglecting the possibility of a climb, one finds that the glide of dislocation, that is the mass-conservative motion *along* the Burgers vector, is determined by a force component,

$$f_b = f_k b_k / |b| = -\sigma b_x b_y / |b| = -\sigma |b| \sin \theta \cos \theta = -\frac{1}{2} \sigma |b| \sin 2\theta \quad (2)$$

where θ is the angle between the Burgers vector and the circumference of the cylinder (Fig. 1). In an isotropic material, the greater this force is the more energetically favorable is the nucleation of a dislocation and/or its glide in the corresponding direction. In other words, one can represent a uniaxial tension as a superposition of an expansion $\sigma/2$, isotropic locally within the wall, and a shear of a magnitude $\sigma/2$ directed at $\pm 45^\circ$ to the

nanotube axis. The shear component along the Burgers vector of the dislocation is responsible for its glide or nucleation.

2. DISLOCATIONS IN A GRAPHENE WALL

Further, the graphene sheet is not isotropic, and the $\{1011\}$ set of planes, reflecting its intrinsic hexagonal symmetry, determines the three preferential slip "planes" along the closest zigzag atomic packing, oriented at 120° to each other. (We will use the standard crystallographic notations, accepted in three-dimensional graphite for the planes and directions, interchangeable with the indexation common in the nanotube studies, as will appear below.) Therefore, no more than one of these planes can be "inert" with respect to shear (if oriented exactly along the circumference or axis, $\theta = 0$, or at $\theta = 90^\circ$, so that f_b vanishes in the Eq. 2), while the shear components along the other two are non-zero (Fig. 1) and they are prone to the slip. The corresponding "c-axis edge" dislocations, necessary in such slip, are indeed known in graphite. Their dislocation cores consist of a 5-7 pentagon-heptagon pair, and the six possible Burgers vectors $1/3a\langle 2110 \rangle$ have the magnitude $b = a = 0.226$ nm, the lattice parameter. Therefore, the primary nucleated dipole (a degenerate dislocation loop in case of 2D lattice) should have a 5-7-7-5 configuration, a 5-7 attached to an inverted 7-5 core, see Fig. 2. Further, this particular arrangement of atoms is known in fullerene science. Formally, it can be obtained in a graphene sheet (or a nanotube wall) by a 90° rotation of a single C-C bond, often called Stone-Wales (SW) interchange. The energy of such a defect is high and the activation barrier is expected to be high, in accord to the "sessile" character of the c-axis edge dislocations in graphite. (One calculation with Tersoff potential estimates approximately 12 eV, with an appropriately higher activation barrier. Tight binding calculations of the barrier for a similar but inverse process indicate however only 7 eV.) In view of the previous discussion, the most probable direction of the formation of a dislocation dipole corresponds to the intrinsic slip plane with the maximum of Peach-Koehler force. The preferred slip direction depends on the type of nanotube, defined by how the graphene strip is rolled up into a cylinder. It is specified by the vector which becomes the circumference, $c = c_1 a_1 + c_2 a_2$ in the basis standard for nanotubes (see Fig. 5

60064539-110597

further in the application). Then $d=0.078 \sqrt{c_1^2+c_2^2+c_1c_2}$ nm, and the chiral symmetry is conveniently described by the angle $\chi=\arctan[\sqrt{3}c_2/(c_2+2c_1)]$, indicating how far the circumference departs from the leading zigzag motif. We use the same basis to present the Burgers vectors as the pairs of integers, (b_1, b_2) , and get from Eq. 2,

$$Fb = \sigma a \frac{\{\sqrt{3}[b_1c_1+b_2c_2+1/2(b_1c_2+b_2c_1)](b_1c_2-b_2c_1)\}}{\{2(b_1^2+b_2^2+b_1b_2)\}^{1/2}(c_1^2+c_2^2+c_1c_2)}$$

$$= (\sqrt{3}/2) [\sigma a^3/(nd)_2] [b_1c_1 + b_2b_2 + 1/2 (b_1c_2 + b_2c_1)] (b_1c_2 - b_2c_1), \quad (3)$$

The max $|f_b|$ defines the most likely slip. Only the smallest Burgers vectors are realistic, $\pm(1,0)$, $\pm(1,0)$ or $\pm(1,-1)$, as we assumed in the last, simplified expression in Eq. 3. Further, all non-equivalent types of nanotubes can be described by the pairs with $0 \leq c_2 \leq c_1$ limited to a wedge on the lattice within the chiral angle $0 \leq \chi \leq 30^\circ$. With this constraint, by directly comparing the values of $|f_b|$ one can see that the choice narrows down to the $\pm(0,1)$ dislocations, that is specifically oriented 5-7 defects, in the language common for fullerenes.

3. STRAIN RELIEF BY THE GLIDE OF "EXTRINSIC" 5-7'S

We can now estimate the energy gain when the externally applied height strain in the nanotube is relaxed by the dislocation glide. A one-step displacement of the 5-7 dislocations is achieved by the SW-rotation of one of the bond, namely the shoulder-bond on the "head-and-shoulders" outline of an isolated 5-7 shape. It can be seen that the corresponding step-displacement is in the direction of the Burgers vector, as it always must be for a conservative (no atomic diffusion, as opposed to *creep*) dislocation movements. The magnitude of this step is one lattice parameter, a . One interesting feature of such glide is due to mere cylindrical geometry of the nanotube-"monocrystal": the glide plane in this case is actually a helix wrapped around the nanotube wall. Similarly, the extra-plane is just a row of atoms also curved into a helix. The dislocation

line (only a monolayer long) is the local normal to the wall of the nanotube, an analog of c-axis [0001] in a graphite crystal.

The force on the $\pm(0,1)$ dislocation can be found from Eq. 3 or simply by noticing that the angle between this Burgers vector and the circumference differs from the chiral angle of the nanotube by 30° , $\theta = \pi/3 - \chi$. Correspondingly, the energy release $f_b a$ equals,

$$\delta E(\epsilon) = -a^2 C/2 \cdot \sin(2\chi + \pi/3) \cdot \epsilon \approx -64.7 \cdot \sin(2\chi + \pi/3) \cdot \epsilon \text{ (eV)}, \quad (4)$$

Here we used the relation $\sigma = C\epsilon$, with the graphene sheet in-plane stiffness $C = 342$ N/m, derived from the Yung modulus of 1020 GPa and interlayer spacing 0.335 nm in graphite. Therefore, the coefficient in Eq. 3 is replaced by its value $a^2 C/2 \approx 64.7$ eV. This numerical value is as accurate as the graphene parameters, less the changes due to the tube curvature. more important is that the energy released is proportional to the applied strain, with the *chirality-dependent* coefficient. This allows a comparison of the yield in different imperfect nanotubes containing small number of statistically oriented dislocations, retained there from the growth process, but not created by the high strain itself (we call them here *extrinsic* for that reason). In this case of course the chirality should be understood in some average sense $\chi = \langle \chi \rangle$ over the large length of the molecule: every 5-7 insertion changes the chiral vector by one unit as will be discussed later, Sec. 5. Similar dependence, although with a smaller coefficient (often between one and three quarters, according to the Polyanyi-Semenov rule in chemical kinetics), should hold for the activation barriers. Summing up, and using the standard methods of the linear transport theory to estimate the flux of 5-7 dislocations, one finds the relaxation rate,

$$\partial \epsilon / \partial t \propto -\sin(2\chi + \pi/3) \cdot \epsilon, \quad (5)$$

The relations (4) and (5) provide the basis for the constituent equations of high-temperature plasticity for any nanotube-material. They indicate that the achiral tubes

must be most resistant, while those chiral with $\chi \approx 15^\circ$ are the "weakest"; the armchair and zigzag are approximately the same in their resistance to static load (however, see Sec. 4). Let us emphasize that this conclusion is drawn with the assumption that there are preexisting 5-7 dislocations, the extrinsic carriers of this plastic flow.

4. NUCLEATION OF THE "INTRINSIC" 5-7 CORES

In case of *molecularly perfect* structure, with none or negligibly few 5-7 insertions, the limiting process for the yield and failure is their *nucleation*, that is the prime Stone-Wales transformation in the pristine hexagonal wall. There are three energetically non-equivalent SW rotations under strain, according to the three orientations of the bonds, in (1,1) (-2,1) and (1,-2) directions. Their energetics for the tube of given chirality should be compared. Topologically, the SW defect is identical to any of the two possible dipoles of dislocations, as Fig. 2 illustrates. Geometrically, however, it has higher symmetry than each of the dipoles, and in order to preserve the intrinsic D_{2h} symmetry of the SW defect, the base approximation is to treat it as a superposition-sum of these two dipoles: the strain in the lattice is a half-sum of the strain-fields produced by each of the constitute dipoles, and so is the strain-relaxation due to SW-transform,

$$E(1,1) = \frac{1}{2}[E_+(1,0) + E(0,1)] \approx \sigma a_0 \sqrt{3/4} \cos(2\alpha) \propto 4c_1 c_2 + c_1^2 + c_2^2 \quad (6a)$$

$$E(-2,1) = \frac{1}{2}[E_-(1,0) + E_+(1,-1)] \approx \sigma a_0 \sqrt{3/4} \cos[(2(\alpha+2\pi/3))] \propto c_1^2 - 2c_2^2 - 2c_1 c_2 \quad (6b)$$

$$E(1,-2) = \frac{1}{2}[E_-(0,1) + E_-(1,-1)] \approx \sigma a_0 \sqrt{3/4} \cos[(2(\alpha+4\pi/3))] \propto c_2^2 - 2c_1^2 - 2c_1 c_2 \quad (6c)$$

Here the integer arguments in the left-hand part specify the orientation of the SW-switched bonds, and the arguments in the right-hand side are the slip directions. The subscript (+ or -) indicates if the dislocations slip in the same or opposite direction as their Burgers vectors. The angle α between the (1,1) bond and the circumference is related to the chirality angle, $\alpha = \pi/6 - \chi$. For the standard representative interval $0 \leq \chi \leq \pi/6$, the rotation of the (1,1)-directed bond gains more relaxation, and one finds,

$$E(1,1) = -C a s_0 \sqrt{3/4} \sin(2\chi + \pi/6) \cdot \epsilon,$$

With this, the energy of the SW transformation can be written,

$$E_{sw}(\epsilon) = E_{sw}(0) - \epsilon \cdot [A + B \sin(2\chi + \pi/6) + \dots],$$

the first term representing the formation energy in a free lattice (as mentioned in Sec. 2), and the important strain-dependent part contains isotropic (due to possible non-zero dilation in the SW) and the leading symmetry-dependent term. The numerical estimate of B is interesting, as it defines how different in yield the nanotubes can be. Unlike the size of the step in the single 5-7 dislocation glide, the size of the prime slip $s_0 = 1/2$, as can be seen by inspection of the changes in the lattice topology. Instead of a hexagonal lattice, Fig. 3 shows a simplified version, the glide direction and a series of atomic planes perpendicular to this glide. With this, we obtain from Eq. (7) $B \approx 28.0$ eV. (One can roughly assess the dilation term, using the evidence of 5% lower density in pentaheptite, that is effective area expansion of 0.01 nm^2 , to be below $A \approx 20$ eV.) The numerical coefficient has to be treated with caution, but the more important dependence on the type of the nanotube follows from the symmetry. We conclude that the molecularly-perfect, pristine nanotubes are the strongest in their zigzag arrangement: SW transformation gains less relaxation energy than the similar defect in an armchair wall.

5. CASE STUDY OF THE (10,10) MOLECULE

Let us consider a (10,10) nanotube, produced in almost pure form by a conventional laser ablation method (We will also see below that this armchair type results in a more general scenario of relaxation.) The initial slip occurs by rotating a bond originally oriented along the circumference, that is a dipole $\pm(0,1)$ [or equivalently $\pm(1,0)$; a similar degeneracy takes place for another achiral type – zigzag – where any of the two bonds oriented at 30° to the circumference can rotate with equal probabilities]. The emerged geometry can be viewed as either a dislocation dipole or a tiny crack along the tubule azimuth (Fig. 4). Once “unlocked”, the SW defect can ease further relaxation. At this stage, both brittle (crack extension) or plastic (separation of dislocation cores and their glide in opposite directions) routes are possible, the former usually at lower and the latter at very high temperatures.

Formally, both routes correspond to a further sequence of SW-switches. The 90° rotation of the strictly azimuthally oriented bonds will result in a 7-8-7 defect (we omit the pentagons appearing on both sides of a crack) and further 7-8-8-7 *etc.*, Fig. 4. Clearly, this will increase the strain of the bonds oriented along the tube axis, and will eventually lead to their breakage with the formation of larger openings, like

$$7-7 \rightarrow 7-14-7 \rightarrow 7-14-8-7 \rightarrow 7-14-8-7 \rightarrow 7-20-7 \rightarrow \dots, \quad (9)$$

accompanied by delocalization of the released electrons. The presence of pentagons on the sides of the crack can result in the curling of the edges. the breakage of the bonds at the crack sides, those belonging to the pentagonal rings, can lead to a pullout of monoatomic chains, as observed in the fast-strain fracture. If the crack, represented by this sequence surpasses the critical size (a molecular analog of the Griffith criteria), it leads to the cleavage of the tubule.

In the more interesting alternative, the SW-rotation of another bond divides the 5-7 and 7-5, as a direct inspection shows, which become the two dislocation cores separated

60064539 110597

by a single row of hexagons (Fig. 4). A next similar SW-switch results in a double-row separated pair of the 5-7, and so on. This leads, at high temperatures, to a plastic flow *inside* the nanotube-molecule. Indeed, a further simplest repetition shows how 5-7 and 7-5 twins glide away from each other driven by the Peach-Koehler elastic forces. Their slow thermally-activated Brownian walk proceeds along these well-defined trajectories. Similarly, their extra-planes are just the rows of atoms also curved into the helices.

When the dislocations sweep a noticeable distance, they leave behind a tube segment changed strictly following the topological rules of dislocation theory. For the new chirality vector c' one finds $(c_1', c_2') = (c_1, c_2) - (b_1, b_2)$, with the corresponding reduction on diameter. While the dislocations of the first dipole glide away, a generation of another dipole may result in further narrowing and proportional elongation under stress, thus forming a neck. The type of a generated dislocation dipole is determined every time by the Burgers vectors closest to the lines of maximum shear (the $\pm 45^\circ$ cross at the end-point of the current circumference-vector c in Fig. 5, in accord with Eqs. 6. Fig. 5 shows geometrically the progression of the chirality vector c , defining the current molecular symmetry, which allows to identify the next state by a simple slip-force construction. The evolution of a (10,10) tube will be:

$$\begin{aligned} (10,10) \rightarrow (10,9) \rightarrow (10,8) \rightarrow \dots \rightarrow (10,0) \rightarrow (9,1) \text{ or } (10, -1)] \rightarrow \\ \rightarrow [(8,1) \text{ or } (9,-1)] \rightarrow (8,0) \rightarrow [(7,1) \text{ or } (8,-1)] \rightarrow (7,0) \text{ etc.} \end{aligned} \quad (10)$$

Interestingly, it abandons any armchair symmetry (c,c) entirely, but then the relaxation oscillates in the vicinity of zigzag (c,0) type, which appears to be a peculiar "attractor". Correspondingly, the diameter changes stepwise, $d=1.36, 1.29, 1.22, 1.16$ nm, etc., the local stress grows in proportion and this "quantized" necking can be terminated by a cleave at late stages.

6. RELATED ASPECTS

Interestingly, such plastic flow is accompanied by the change of *electronic structure* of the emerging domains, governed by the vector (c_1, c_2) : armchair tubes being metallic, and others – semiconducting with the different band gap values. The 5-7 pair separating two domains of different chirality has been proposed to be a pure-carbon heterojunction. Here we have shown that this electronic heterogeneity can arise from a mechanical relaxation: if the initial tube was metallic (armchair), the plastic dilation transforms it in a semiconducting types irreversibly [Sec. 5, Eq. (10)].

The dislocation motion in the nanotube wall differs critically from a regular three-dimensional case. Here we have one-dimensional objects drifting (a process both thermally activated and driven by the applied stress) along the well-defined helical trajectories. There is almost no entanglement of the dislocation lines – a usual cause of materials work-hardening. Principally, this low-dimensional nature makes the plasticity more “reversible” (Especially in the light of Kac theorem, the cores-twins diffusing in the one-dimensional compact tend to re-collide and annihilate), if the stress is removed in the sufficient annealing process. In the other hand, change of chirality from (c, c) toward zigzag type $(c, 0)$ results in a *work-hardening* of entirely different nature, special for nanotubes only; the change in the formation and activation energies described above results in a significant variation of the tubule response to further load.

A nanotube with a 5-7 dislocation core in its wall does not possess an axial *symmetry* and is expected to relax into a somewhat bent shape. For instance, the calculation typically shows that a junction of an $(8, 0)$ with a $(7, 1)$ tube, which requires a single 5-7 insertion, has an equilibrium angle up to 15° . Interesting then, an exposure of an even achiral nanotube to the axially symmetric tension results in a formation of two 5-7 dislocations, and when the tension is removed, the tube “freezes” in a somewhat asymmetric configuration, S-shaped or C-shaped, depending on the time of exposure, Fig. 6. Of course the symmetry is preserved statistically, since many differently distorted shapes can form under identical conditions.

The issue of nanotube tensile *strength* is especially important: the mere combination of the strongest bonds in a no-edge and low defect arrangement does suggest a record strength per unit of weight and invites a variety of applications. Therefore

further theoretical analysis should be based on the kinetic theory combined with the most accurate modeling of the elementary steps (since $kT=0.03$ eV makes the kinetics sensitive). Accurate activation enthalpies and the comparison of the kinetic rates of different elementary steps, will provide further details for the described mechanisms, their non-equilibrium thermodynamics and, in more practical terms, the strength limits and the degradation paths for fullerene nanotubes (we do not even approach here possible chemical attack combined with high strain). This should be done with appropriate care and in a due pace, "for Nature cannot be fooled".

It is interesting to mention the evidence of almost-reversible cyclic "folding" of a nanotube, with the reported small residual strain after the 16% local tension in the outward side of the bend. Possibly it retains a few of forced plastic imperfections, described above, not easily annealed at ambient temperature. In the other, more controllable experiment, a *bending* strength was measured explicitly. Its low value is due to the delamination of the layers in the multiwall nanotube, on the compression side (as for example in TEM images). To calculate such bending strength theoretically, we can use the shell model, with the effective thickness $h=0.08$ nm. The delamination-buckling event in this case can be approximated as a buckling of an elastically-supported ($C_{33} > 0$) plate (Fig. 7), as described by the forth-order ODE,

$$Y_s I_s Z^{iv} + c \cdot \sigma_{\text{compr}} Z'' + (C_{33}/c) Z = 0, \quad (11)$$

Here $c=0.34$ nm, $Y_s h \approx C_{11} \cdot c$, the moment of inertia $I_s = h^3/12$, and Z is the deviation of the outmost layer from its normal position at the distance c from the nearest neighbor. (We use here standard for graphite values $C_{11}=1$ TPa and $C_{33} = 36$ GPa, reflecting the soft van der Waals interlayer forces.) The first bifurcation can be found then to occur at $\sigma_{\text{compr}} =$

$(h/\sqrt{3c}) \sqrt{C_{11} C_{33}} \approx 26$ GPa. This is an excellent agreement with the reported values (14.2 ± 8.0 GPa, with the greatest detected 28.5 GPa), in spite of possible effects of the overall cylindrical curvature. Bifurcations are notoriously sensitive to the minor influences, which makes – in this case – the large spread of values an almost encouraging feature.

The analysis which is described by the invention applies concepts of macro-plasticity and fracture theory to carbon nanotube (CNT) response to extreme tension. It reveals the possibility, under very high tension and temperature, of plastic flow which at certain conditions leads to a "quantized" stepwise necking: the CNT diameter changes by the discrete fractions, while the tube elongates in proportion. At lower temperatures, the relaxation begins as a brittle cleave in the azimuthal direction.

The analysis may be carried out in several steps. First, the uniaxial strain p is presented as a mathematical superposition of a uniform expansion $p/2$ (both at 45° with respect to the CNT axis). Second, we note that the shear components of high amplitude should generate the dislocation dipoles. The Burgers vectors in such dipole b and $-b$ and, in case of archetypal (10,10) tube serving as example, are oriented at 60° with respect to the CNT axis. Third, the same shear stress forces these dislocations to separate and glide away from each other. The core structure of each dislocation, known as edge-nonbasal, e.g., $(0111)a/3[2110]$, is pear-shaped, 5-7 pentagon-heptagon pair, $b=0.246$ nm. Therefore, the initially formed dipole pair (b and $-b$ next to each other), as a single defect in a graphite wall of a nanotube, consists of 2 heptagons and 2 pentagons. Such defects have been known to exist in C60, graphite, and in nanotubes, formed by a simple 90° rotation of a single C-C bond. Relatively small (per 24 atoms) energy ensures low activation barrier of their formation. This barrier is further reduced by the tension. Fourth, when this atomic arrangement is formed, it manifests a duality of being a dislocation dipole (precursor of plasticity), and/or a tiny 0.71 nm long Griffith crack (precursor of brittle cleave). There are two possible paths for further evolution, both involving a Stone-Wales transformation—a rotation of one of the C-C bonds. Rotation of the bond adjacent to the dipole on the CNT azimuth, results in a crack growth (7-8 pair forms, then 8-8, and a larger 14-whole, etc.) in a brittle scenario. The rotation of the external "shoulder"-bond in any of 5-7 pair leads to the separation of the dislocations, gliding and plastic relaxation. The comparison of the energetics of these defects allows the type of proceeding relaxation to be mapped on a p - T diagram. Remarkably, the plasticity resulting from a glide of emerging dislocations along the helical paths results in a certain change of helicity. More particularly, the helicity of the CNT section between

the two running away edge-dislocations differs from the initial gliding pair, and elongates. Further, evolution is a result of competition of the energetics (under a given p and T) of the glide and the birth of a new dislocation-dipole in the narrower (and therefore more stressed) section.

The change of chirality from (c,c) toward zigzag type $(c,0)$ can lead to a work-hardening of an entirely different nature which is specific for nanotubes. The change in the formation and activation energies, presumably due to the change in the orientation of the hexagonal lattice with respect to the direction of tension and shear, can result in a significant variation of the tubule response to further load.

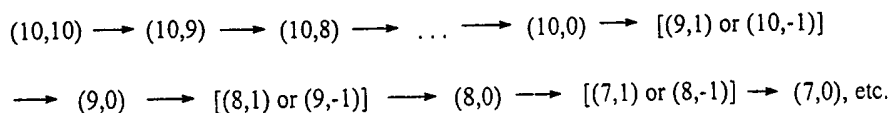
In accordance with the invention, the deliberate change in nanotube helicity can have a profound effect on various mechanical, optical, and electronic properties and thus is desirable.

7. EXAMPLE

A $(10,10)$ nanotube produced by a laser ablation method can be modified into a chiral-type $(10,9)$ nanotube. The nanotube is exposed simultaneously to a combined high temperature and mechanical load. The thermal treatment can range from 1500°C to 2500°C . The thermal treatment may be enhanced by employing light irradiation, an electron beam, and the like. As an example, the thermal treatment can be 2000°C in the absence of light. This enhancement may be desirable since it is expected to significantly facilitate formation and glide of dislocations, responsible for the change of nanotube helicity. The activation barrier for the Woodward-Hoffman forbidden Stone-Wales rotations may be significantly reduced by photon absorption.

The stress range of the mechanical load preferably ranges from 10 GPa to 60 GPa, more preferably from 10 GPa to 30 GPa. The average elastic modulus for a rope packing of nanotubes is typically 600 GPa. The stress range of the mechanical load corresponds to tensile forces applied to individual tubes in the range of 0.1 micro-newtons. The above stress load is usually applied as a tensile stress. It should be noted, however, that the tensile stress may be replaced by torsion, which is capable of creating shear in another direction, leading therefore to a different change of nanotube helicity.

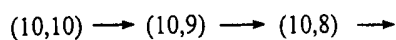
A general relaxation path (i.e., the sequence of the helicities of the forming nanotube segments) can be expressed as:



The time of treatment, along with the temperature and stress values, can be altered to obtain the product which is desired. Typically, the time ranges from minutes to hours. In general, if lower temperature and stress values are used, it may be preferable to utilize a higher time of treatment relative to using higher temperature and stress values.

In view of recent findings, the forming of hetero-junctions, i.e., joint nanotube segments with different helicities, can be of special interest since they may form nanoscale electronic devices with nonlinear characteristics.

In accordance with the invention, under proper conditions, one can gradually vary the helicity of CNT, e.g., as presented by reaction steps



.... or (9,9) and so on. The exact sequence of helicities can be identified by application of the Peach-Koehler formula or its analogs, to estimate which of the two possible dislocation pairs will be preferential [(b,-b) or the rotated by 60 degree pair(b,-b)]. This "necking" process, if continued, leads to an increase of local stress and final cleavage, with possible atomic chain pull-out at high stress rates, as it takes place in some other materials and in greater lengthscale. This may constitute an important technological application in manufacturing CNTs of different helicities.

The change in helicities is able to change the electronic properties of the tubes. It is therefore remarkable and unexpected that the plastic flow in molecular scale leads to electrical heterogeneity, where dislocation core separates the domains of possibly metal and semiconductor. Another unique feature may be attributable to the lack of dislocation lines in 2D space. Accordingly, they do not become tangled, and one should not work-hardening (increase of mechanical resistance with the amount of strain), which may be widespread in many materials. For the same reason, the intramolecular plasticity is

theoretically reversible: applying the opposite strain (compression) under annealing conditions, one can force the dislocations to glide backward along exactly same paths and annihilate with their own anti-twins. 5051-416.app

265011-6E549009

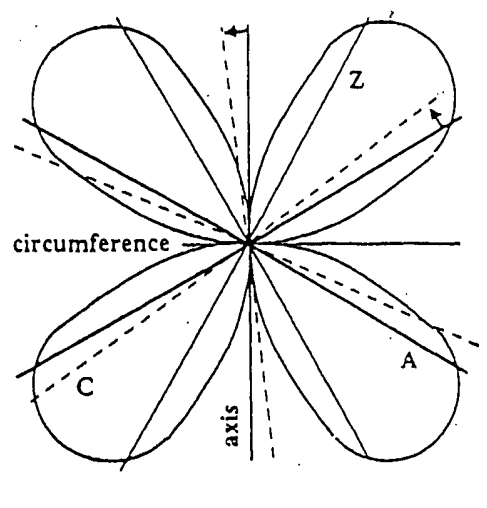


Fig. 1 A "clover-leaf" angular distribution of the shear stress resulting from the uniaxial tension (maximums at $\pm 45^\circ$). The straight beams indicate the intrinsic glide planes in the hexagonal lattice of the nanotube: armchair (A, thick solid), zigzag (Z, thin solid), and arbitrary chiral (C, dashed). As a result of the 5-7 glide, forced by the great strain, the tube changes its helicity, and the internal glide planes rotate gradually from the armchair (A), through a chiral (C), to the zigzag (Z) type. The relative position of the glide planes with respect to the shear field determines the yield resistance of the nanotube as discussed herein.

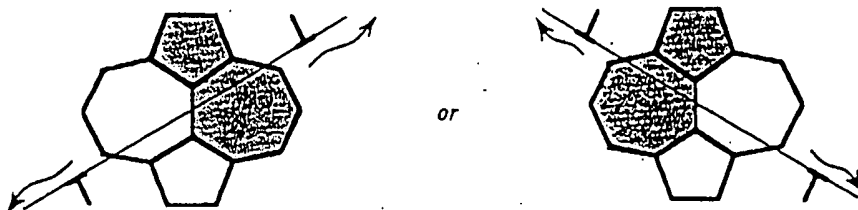


Fig. 2 Stone-Wales configuration is topologically identical to the dipole of Roscoe-Thomas 5-7 dislocations. Two possible choices correspond to the different glide planes. Geometrically SW has the symmetry higher than each of the dipoles separately. Correspondingly, the SW energy is estimated in Eq. 6 as a half-sum of that for the dipoles.

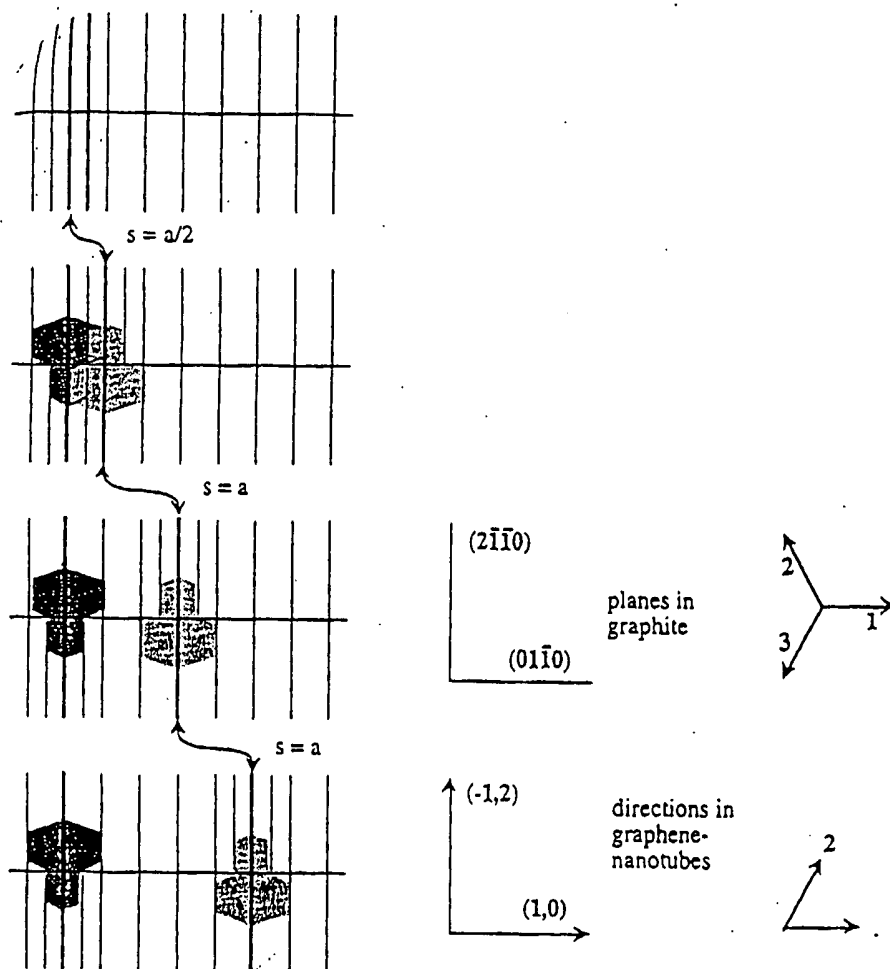


Fig. 3 A simplified version of the honeycomb hexagonal lattice. It shows only one glide plane $(01\bar{1}0)$, and the atomic planes perpendicular to it $(2\bar{1}\bar{1}0)$ [In the "nanotube" notations these are directions-vectors $(1,0)$ and $(-1,2)$ correspondingly.] The spacing between the drawn planes is of no importance, it should of course be relaxed remotely from the dislocation cores to the constant equilibrium spacing, $a/2$ in this case. It is clear that the original slip – the first stone-Wales transformation – corresponds to the dislocation displacement by $a/2$ from each other, while a regular step in dislocation glide is always a .

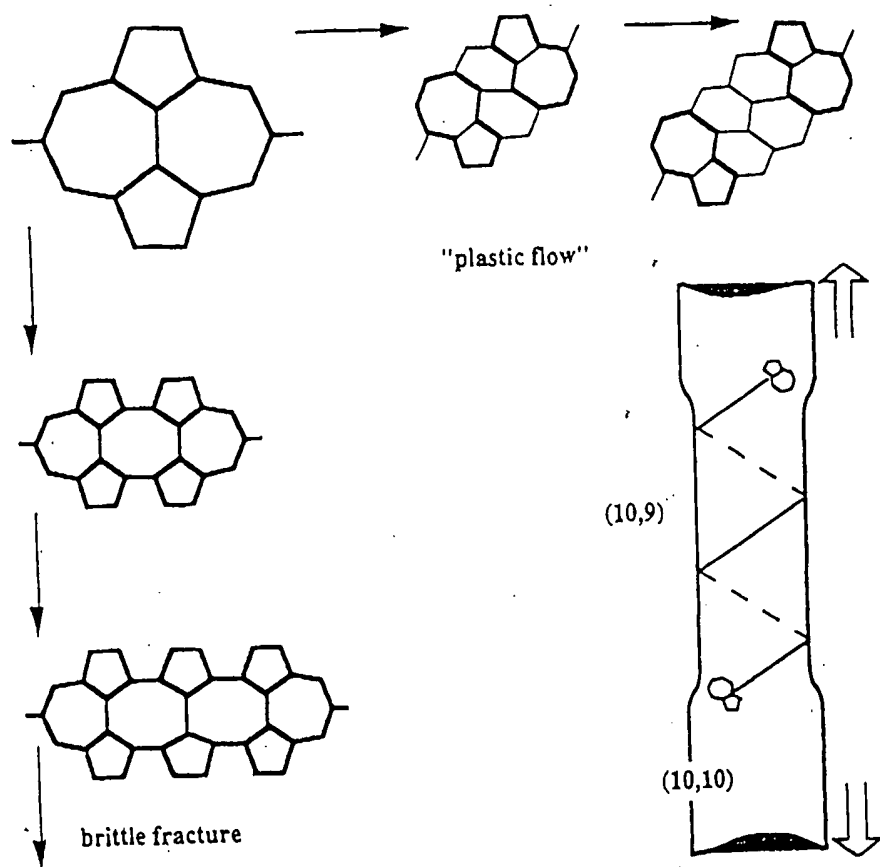


Fig. 4 A tiny "dislocation loop" nucleated in the two-dimensional wall of a nanotube is represented by the two opposite Burgers vectors, each corresponding to a 5-7 pair. The formed 5-7-7-5 configuration evolves further as either a crack (brittle cleavage) or as a couple of dislocations gliding away along the spiral "slip plane" (plastic yield). In the latter case, the change of the nanotube helicity is reflected in a stepwise change of diameter and the corresponding variations of electrical properties.

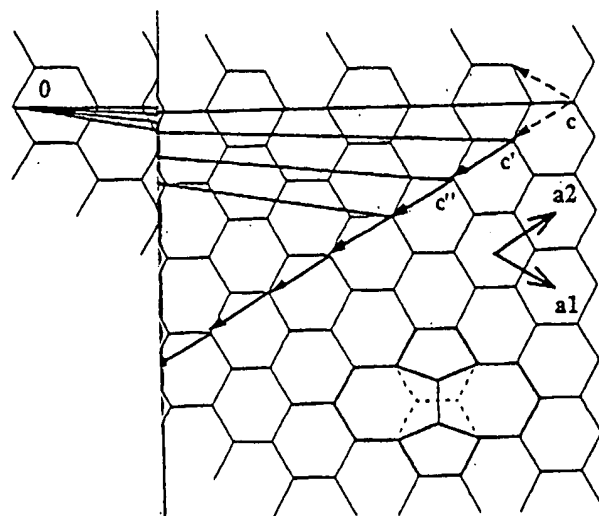


Fig. 5 The dynamic progression of the nanotube chirality (vector c) can be traced with the use of this construction. The horizontal line indicates the initial circumference mapping on the flat hexagonal lattice. The short arrows are the Burgers vectors of the generated dislocations, and are always chosen as close as possible to the $\pm 45^\circ$ with respect to the current c -circumference, to ensure the best energy gain. The dashed arrows correspond to the situations with degeneracy, when the two types of glide are equally probable. Also shown is the unrelaxed Stone-Wales pattern, and the standard basis vectors, a_1 and a_2 .

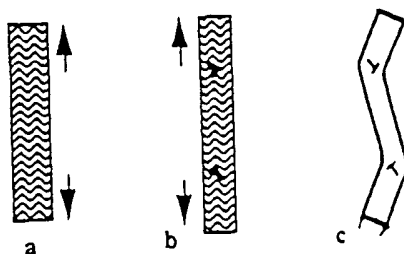


Fig. 6 Symmetry breaks while the nanotube does not: an exposure of a symmetric achiral nanotube (a) to the strictly axial forces (at high temperature) generates a pair of 5-7 dislocations (b). After such symmetric operation is over, the forces are removed and the nanotube freezes in an asymmetric shape, for example S-curved (c).

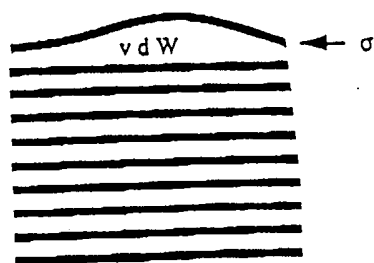


Fig. 7 The most compressed external graphene layer on the inward side of the bend buckles while being supported by the van der Waals interactions with the rest of the stack.

REQUEST FOR ACCESS TO AN APPLICATION UNDER 37 CFR 1.14(e)

RECEIVED

OCT 04 2002

File Information Unit

In re Application of

Yakobson

Application Number

601064,539

Filed

11/05/97

Art Unit

Examiner

Paper No. #2

Assistant Commissioner for Patents
Washington, DC 20231

1. ☒ I hereby request access under 37 CFR 1.14(e)(2) to the application file record of the above-identified ABANDONED Application, which is not within the file jacket of a pending Continued Prosecution Application (CPA) (37 CFR 1.53(d)) and is: (CHECK ONE)

☐ (A) referred to in:

United States Patent Application Publication No. 6280,677, page _____, line _____

United States Patent Number _____, column _____, line _____, or

an International Application which was filed on or after November 29, 2000 and which

designates the United States, WIPO Pub. No. _____, page _____, line _____.

☐ (B) referred to in an application that is open to public inspection as set forth in 37 CFR 1.11(b) or

1.14(e)(2)(i), i.e., Application No. _____, paper No. _____, page _____, line _____.

2. ☐ I hereby request access under 37 CFR 1.14(e)(1) to an application in which the applicant has filed an authorization to lay open the complete application to the public.

Azriel Tesfay
Signature

Azriel Tesfay
Typed or printed name

10/4/02

Date

RECEIVED

FOR PTO USE ONLY

OCT 04 2002

Approved by: *gm*

(Initials)

File Information Unit

70556 U.S. PTO

60/064539



PATENT APPLICATION SERIAL NO. 11/05/97

U.S. DEPARTMENT OF COMMERCE
PATENT AND TRADEMARK OFFICE
FEE RECORD SHEET

04/02/1998 CROBINS 00000004 DAN:500220 60064539
01 FC:114 75.00 CH 75.00 DP

01/21/1998 JBATTS 00000067 60064539
01 FC:214 75.00 DP

Adjustment date: 04/02/1998 CROBINS
01/21/1998 JBATTS 00000067 60064539
01 FC:214 -75.00 DP

PACE DATA ENTRY CODING SHEET

U.S. DEPARTMENT OF COMMERCE
Patent and Trademark Office

1ST EXAMINER
2ND EXAMINER

DATE
DATE

APPL NO. 11/05/97

PTO NUMBER

TYPE APPL

FILING DATE
MONTH DAY YEAR

SPECIAL HANDLING

GROUP ART UNIT

CLASS

SHEETS OF DRAWING

TOTAL CLAIMS

INDEPENDENT CLAIMS

SMALL ENTITY?

FOREIGN LICENSE

FILING FEE

ATTORNEY DOCKET NUMBER

CONTINUITY DATA

CONT STATUS CODE

PARENT APPLICATION SERIAL NUMBER

PCT APPLICATION SERIAL NUMBER

PARENT PATENT NUMBER

PARENT FILING DATE

FOREIGN PRIORITY CLAIMED

COUNTRY CODE

PCT/FOREIGN APPLICATION SERIAL NUMBER

FOREIGN FILING DATE

PCT/FOREIGN APPLICATION DATA

U.S. DEPARTMENT OF COMMERCE
Patent and Trademark Office

PACE DATA ENTRY CODING SHEET

1ST EXAMINER
2ND EXAMINER

DATE
DATE

APPLICATION NUMBER	60/064539	TYPE APPL	9	FILING DATE	MONTH	DAY	YEAR	SPECIAL HANDLING	GROUP ART UNIT	CLASS	SHEETS OF DRAWING
					11	05	97				6
TOTAL CLAIMS	2	INDEPENDENT CLAIMS		FILING FEE	75	FOREIGN LICENSE			ATTORNEY DOCKET NUMBER		
									5051416		

Handwritten signature

CONTINUITY DATA

CONT STATUS CODE	PARENT APPLICATION SERIAL NUMBER	PCT APPLICATION SERIAL NUMBER	PARENT PATENT NUMBER	PARENT FILING DATE	
MONTH	DAY	YEAR	MONTH	DAY	YEAR
		P C T /			
		P C T /			
		P C T /			
		P C T /			
		P C T /			

PCT/FOREIGN APPLICATION DATA

FOREIGN PRIORITY CLAIMED		COUNTRY CODE		PCT/FOREIGN APPLICATION SERIAL NUMBER		FOREIGN FILING DATE	

[illegible]

ATTORNEY REGISTRATION NUMBERS

[illegible]

CORRESPONDENCE NAME AND ADDRESS

[illegible]

APPLICANT/INVENTOR DATA

[illegible]

POSITION		ID NO.	DATE
CLASSIFIER			
EXAMINER		66068	4-8-98
TYPIST			
VERIFIER			
CORPS CORR.			
SPEC. HAND			
FILE MAINT			
DRAFTING			